Submitted to Geophysics

LBL-10378
Preprint

A HYBRID 3D ELECTROMAGNETIC MODELLING SCHEME

K. H. Lee, D. F. Pridmore, and H. F. Morrison

January 1980

Prepared for the U. S. Department of Energy
under Contract W-7405-ENG-48

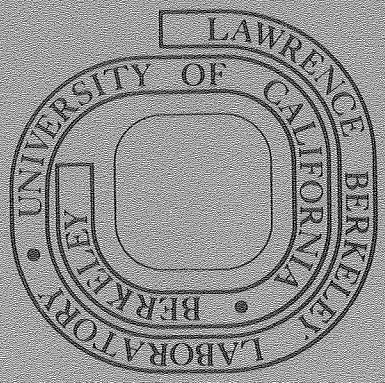

DISCLAIMER

Submitted to Geophysics.

LBL-10378

A HYBRID 3D ELECTROMAGNETIC MODELLING SCHEME

K. H. Lee,* D. F. Pridmore,† and H. F. Morrison*

Lawrence Berkeley Laboratory
University of California
Berkeley, California 94720

*Engineering Geoscience
University of California
Berkeley, CA 94720

†Western Mining Corporation
Exploration Division
55 MacDonald Street
Kalgoorlie, W. A., Australia 6430

Table of Contents

List of Figures

A HYBRID 3D ELECTROMAGNETIC MODELLING SCHEME

K. H. Lee,* D. F. Pridmore,† and H. F. Morrison*

Abstract

This paper presents an efficient numerical method for the electromagnetic scattering of arbitrary three-dimensional local inhomogeneities buried in a uniform or two-layered earth.

In this scheme the inhomogeneity is enclosed by a volume whose conductivity is discretized by a finite element mesh and whose boundary is only a slight distance away from the inhomogeneity. The scheme uses two sets of independent equations. The first is comprised of finite element equations derived from a variational integral, and the second is a methematical expression for the fields at the boundary in terms of the electric fields inside of the boundary. The Green's function is used in the derivation of the second set of equations. An iterative algorithm has been developed using these two sets of equations. The solutions are the electric fields at nodes inside the finite element boundary. The scattered fields anywhere may then be obtained by performing volume integrations over the inhomogeneous region.

This scheme has been used for modelling three-dimensional inhomogeneities in plane wave and magnetic dipole studies. The results confirm earlier model analyses using the finite element technique.

*Engineering Geoscience, University of California, Berkeley, California.
†Western mining Corp., Exploration Division, 55 MacDonald Street, Kalgoorlie, W. A., Australia 6430.

Introduction

A limited number of numerical solutions for 3D electromagnetic (em) problems has been discussed in geophysical literature. These solutions have been obtained using either the integral equation or finite element (finite difference) techniques. Lines and Jones (1973) and Reddy et al. (1977) have presented solutions to 3D MT problems using finite difference and finite element techniques, respectively. Pridmore (1978) reported iterative solutions to 3D electric and em problems using the finite element technique. The drawbacks of this technique are: 1) the number of equations is so large that the computer cost is prohibitive, 2) numerical derivatives of the obtained solution are not always reliable. These difficulties can be avoided using the integral equation technique provided that the inhomogeneity is of finite extent. The application of the integral equation technique to 3D em problems has been reported by Hohmann (1975), Weidelt (1975), and Meyer (1977). In this technique the number of equations is basically the same as the number of inhomogeneous elements, but the matrix is full and generally asymmetric.

A hybrid scheme was introduced by Scheen (1978) which uses a combination of these techniques. A variational integral in terms of magnetic fields is initially formulated over a region discretized by a finite element mesh. A system of linear equations is derived from the variational integral. Using integral relations, a different set of equations is derived for the scattered magnetic fields at the finite element boundary positioned some distance away from the inhomogeneity. To derive the second set of equations the scattering current must first be found through a numerical $\nabla \times \overline{H}$ operation. An algebraic substitution of the second set of equations into the first set leads to a combined set of linear equations, from which the magnetic fields inside of the

finite element boundary are finally obtained. This is the direct hybrid scheme. The matrix for the combined set of equations is full and asymmetric. The size of the matrix is slightly larger than the one associated with the integral equation technique, but the scheme does not need to evaluate Green's functions between elements within the finite element boundary, thus avoiding the problem of singular cell integration. The second approach discussed by Scheen is an iterative scheme which uses the same sets of equations. Initial field values are assigned along the boundary and the first set of finite element equations is solved. Scattered magnetic fields are then calculated using the second set of equations. These scattered fields are substituted for the boundary fields and the process is repeated iteratively until changes in the boundary values become insignificant.

In the present approach we have solved the problem iteratively in terms of the secondary electric fields within the mesh. The scattering currents can then be obtained directly by adding appropriate primary electric fields to the finite element solutions and by multiplying the results by the anomalous conductivities. This process avoids the difficulty of taking the numerical curl operation which would otherwise be necessary when the solution is derived in terms of magnetic fields.

Formulations of finite element equations and integral relations

Initially, a set of finite element equations is derived from a variational integral. The variational integral may be formulated using either the total electromagnetic energy contained in the system (Morse and Feshbach, 1953) or a mathematical function defined by the minimum theorem (Stakgold, 1968). In this paper the minimum theorem has been applied to derive a system of finite element equations.

Maxwell's equations for an $e^{j\omega t}$ time dependent system become

$$\nabla \times \bar{E} = - \hat{z}\bar{H} - \bar{M}_s \tag{1}$$

and

$$\nabla \times \bar{H} = \hat{y}\bar{E} + \bar{J}_s \tag{2}$$

where $\hat{z} = j\omega\mu$ and $\hat{y} = \sigma + j\omega\epsilon$, and $\bar{M}_s$ and $\bar{J}_s$ are impressed magnetic and electric sources. The domain equation for the electric field in the presence of $\bar{J}_s$ alone is derived from (1) and (2) as

$$\nabla \times \frac{\nabla \times E}{\hat{z}} + \hat{y}\bar{E} = - \bar{J}_s. \tag{3}$$

The minimum theorem provides the corresponding functional to equation (3) as

$$F(\bar{E}) = \int_v \{(\nabla \times \frac{\nabla \times \bar{E}}{\hat{z}} + \hat{y}\bar{E}) \cdot \bar{E} + 2\bar{E} \cdot \bar{J}_s\} dv. \tag{4}$$

This is a variational integral where the operator $(\nabla \times \frac{\nabla \times}{\hat{z}} + \hat{y})$ is self adjoint. It can be shown (Pridmore, 1978) that the solution to equation (3) corresponds to a stationary point of the functional $F(\bar{E})$. Applying the vector identity, $\nabla \cdot \bar{A} \times \bar{B} = \bar{B} \cdot \nabla \times \bar{A} - \bar{A} \cdot \nabla \times \bar{B}$, and the divergence theorem, equation (4) becomes

$$\sum_i [\int_{v_i} (\frac{\nabla \times \bar{E} \cdot \nabla \times \bar{E}}{\hat{z}} + \hat{y}E \cdot E + 2\bar{E} \cdot \bar{J}_s) dv + \int_{s_i} (\bar{E} \times \bar{H}) \cdot d\bar{s}] \tag{5}$$

where the volume has been divided into a number of smaller ones over which σ is constant. The surface integrals along adjacent boundaries must cancel because the tangential components of $\bar{E}$ and $\bar{H}$ are continuous. At the external boundary, the surface integrals will not contribute to the variation of $F(\bar{E})$. With proper boundary values prescribed, the tangential components of either $\bar{E}$ or $\bar{H}$, the variation of $\int_s (\bar{E} \times \bar{H}) \cdot d\bar{s}$ would vanish. Another useful condition commonly encountered is

$\bar{E}\times\bar{H}\cdot\bar{n} = 0$, namely the natural boundary condition. If the electromagnetic fields are either symmetric or antisymmetric across a certain surface, this surface may be called a natural boundary, and no power is transmitted across this surface. Thus, the effective variational integral is the volume integral part of equation (5).

$$F(\bar{E}) = \sum_i \int_{v_i} \left(\frac{\nabla\times\bar{E}\cdot\nabla\times\bar{E}}{\hat{z}} + \hat{y}\bar{E}\cdot\bar{E}+2\bar{E}\cdot\bar{J}_s\right)dv. \tag{6}$$

The functional is in terms of the total electric fields. If we know the primary electric field, the field that would exist in the presence of a horizontally layered half space alone, the functional could alternatively be formulated in terms of the secondary electric fields. According to the principle of superposition, $\bar{E} = \bar{E}_p+\bar{E}_s$, we can derive the domain equation for the secondary electric field as

$$\nabla \times \frac{\nabla\times\bar{E}_s}{\hat{z}} + \hat{y}\bar{E}_s = -\Delta\hat{y}\bar{E}_p \tag{7}$$

where subscripts s and p denote "secondary" and "primary," respectively, and $\Delta\hat{y}$ is the difference in $\hat{y}$ between the medium used for the primary field calculation and the inhomogeneity. The corresponding functional $F(\bar{E}_s)$ can also be written as

$$F(\bar{E}_s) = \sum_i \int_{v_i} \left(\frac{\nabla\times\bar{E}_s\cdot\nabla\times\bar{E}_s}{\hat{z}} + \hat{y}\bar{E}_s\cdot\bar{E}_s+2\Delta\hat{y}\bar{E}_s\cdot\bar{E}_p\right)dv. \tag{8}$$

Using hexahedral elements and a tri-linear base function which describes the field behavior in each element, the secondary electric fields in a particular element e may be approximated by (Zienkiewicz, 1971)

$$\underline{E}_s^e = (N_1 N_2 \cdots N_8)(\underline{E}_{s1}\underline{E}_{s2}\cdots\underline{E}_{s8})^T$$

for each component of the electric fields. The shape function $N_j, j = 1\sim8$, are tri-linear, and $\underline{E}_{sj}, j = 1\sim8$, are the unknown secondary fields at eight corners of a hexahedron. After substituting the approximation into (8), and carrying out volume integrations with continuous stacking of these elementary entries onto a system matrix K, we obtain the following matrix representation for the functional $F(\underline{E}_s)$;

$$F(\underline{E}_s) = \underline{E}_s^T K \underline{E}_s + 2\underline{E}_s^T S. \tag{9}$$

The stationary point of functional F can be found by setting the first derivative of F with respect of $\underline{E}_s$ to zero. The first derivative of F is equivalent to the first variation of F. In either case, a system of matrix equation

$$K\underline{E}_s = -S \tag{10}$$

is generated. This is the finite element equation. The system matrix K is banded and symmetric. For a grid system of 10 x 10 x 10 nodes in each direction, the total number of equations is 3,000 with a maximum half bandwidth of 336 including the diagonal entry. The memory requirement for this system is roughly 1 million complex words. This is about the maximum size for the iterative hybrid scheme for which the economic aspects are practical.

To solve equation (10) we must provide both the primary fields inside of the inhomogeneity and the secondary fields at nodes on the finite element boundary. The primary field solution for a layered half space has been given by Wait (1962), Quon (1963), Frischknecht

(1967), Dey and Ward (1970), and Ryu et al. (1970), to list a few. Using $\bar{A}$ and $\bar{F}$ vectors, Pridmore (1978) derived a solution for a two-layered half space. The hybrid scheme presented here uses the same primary field.

To find the secondary field scattered by an inhomogeneity, let us first consider a point source of current, $\bar{J}^s$, in the lower half space of a two-layered earth. Following Harrington (1961, p. 77), the divergenceless vector $\bar{H}$ is the curl of an arbitrary vector $\bar{A}$, $\bar{H} = \nabla\times\bar{A}$, then, $\bar{A}$ satisfies the following inhomogeneous wave equation in rectangular coordinates;

$$\nabla^2\bar{A} + k^2\bar{A} = -\bar{J}^s\delta(\bar{r}-\bar{r}') \tag{11}$$

where $k^2 = -\hat{z}\hat{y}$, and $\bar{r}$ and $\bar{r}'$ are the positions of observation and source, respectively. The particular solution to (11) is given by

$$\bar{A}^p = \frac{\bar{J}^s}{4\pi}\frac{e^{-jk|\bar{r}-\bar{r}'|}}{|\bar{r}-\bar{r}'|} \tag{12}$$

and fields caused by the particular solution $\bar{A}^p$ are also given by

$$\bar{E}^p = -\hat{z}\bar{A}^p + \frac{1}{\hat{y}}\nabla(\nabla\cdot\bar{A}^p) \tag{13}$$

$$\bar{H}^p = \nabla \times \bar{A}^p. \tag{14}$$

In the presence of horizontal interfaces, we must consider the secondary field caused by the reflections at these boundaries. An appendix is provided to show the derivation of electric field in a two-layered half space and magnetic field in the air. In the integral equation technique the conductive inhomogeneity is simulated by a collection of electric current sources distributed over the volume occupied by the inhomogeneity. This current is called the scattering current and is defined by the product of $\Delta\hat{y}$ and the total electric field

(Harrington, 1961). The true boundary value of the hybrid scheme is the secondary field due to the inhomogeneity. Therefore, the boundary value is the volume integral of the electric field given by (A-18) with $\bar{J}^s(\bar{r}')$ replaced by $\Delta\hat{y}(\bar{r}')\{\bar{E}_p(\bar{r}') + \bar{E}_s(\bar{r}')\}$. Thus,

$$\bar{E}_s(\bar{r}) = \int_v \bar{\bar{\Gamma}}^E(\bar{r};\bar{r}')\cdot\Delta\hat{y}(\bar{r}')\{\bar{E}_p(\bar{r}') + \bar{E}_s(\bar{r}')\}dv. \tag{15}$$

Using the same grid system that gives rise to the finite element equation (10), we can approximate the integral (15) by

$$\bar{E}_s(\bar{r}) = \sum_i \int_{v_i} \bar{\bar{\Gamma}}^E(\bar{r};\bar{r}')\cdot\Delta\hat{y}(\bar{r}')\{\bar{E}_p(\bar{r}') + \bar{E}_s(\bar{r}')\}dv \tag{16}$$

where $\Delta\hat{y}(\bar{r}')$ is assumed to be a constant in each hexahedron. Then the scattered field at the boundary may be written in a matrix form as

$$\underline{E}_s^b = G\underline{E}_s^i + S_p \tag{17}$$

where superscripts b and i denote "boundary" and "inhomogeneous region," respectively, and S_p is an additional source vector due to the primary field. G is an m×n matrix whose entries may be obtained by integrating $\bar{\bar{\Gamma}}^E(\bar{r};\bar{r}')\ N(\bar{r}')$ over each elementary volume. Here, $N(\bar{r}')$ is the same shape function used for the derivation of the finite element equation (10), and m and n are the numbers of nodal points on the boundary and inside of the boundary, respectively. If we partition the finite element equation (10) into

$$\begin{pmatrix} K_{ii} & K_{ib} \\ K_{bi} & K_{bb} \end{pmatrix}\begin{pmatrix} \underline{E}_s^i \\ \underline{E}_s^b \end{pmatrix} = -\begin{pmatrix} S_i \\ S_b \end{pmatrix} \tag{18}$$

then the upper part of equation (18) is

$$K_{ii}\underline{E}_s^i + K_{ib}\underline{E}_s^b = -S_i. \tag{19}$$

Substituting equation (17) into (19), we find

$$(K_{ii}+K_{ib}G)\underline{E}_s^i = -(S_i+K_{ib}S_p)$$

and the solution for $\underline{E}_s^i$ becomes

$$\underline{E}_s^i = -(K_{ii}+K_{ib}G)^{-1}(S_i+K_{ib}S_p). \tag{20}$$

This is the direct hybrid scheme for the secondary electric fields inside of the boundary. The matrix $(K_{ii}+K_{ib}G)$ is asymmetric and full, and of order n.

The iterative hybrid scheme is initiated by solving the finite element equation (19) using an initial guess for the boundary values. Thus, the initial secondary field solution becomes

$$\underline{E}_s^i = -K_{ii}^{-1}(S_i+K_{ib}\underline{E}_s^b). \tag{21}$$

A complex version of a direct solution algorithm developed by Reid (1972) has been used. With this initial solution inside of the inhomogeneity, the scattered field is computed at the boundary using equation (17). The volume integral of Green's function is carried out using one- or two-point Gaussian quadrature. The Green's dyadics computed during the first iteration are stored and repeatedly used as iteration is continued.

The weighting associated with the evaluation of new boundary value has been a major problem in this scheme. The boundary value for the ith iteration is given by

$$(\underline{E}_s^b)^i = (\underline{E}_s^b)^{i-1} + W\{\underline{E}_s^* - (\underline{E}_s^b)^{i-1}\} \tag{22}$$

where $\underline{E}_s^*$ is the scattered field given by (17), and W is a weighting coefficient. A number of different values of W has been tested on a simple 3D model. The model is a brick of size 1 km × 2 km × 2 km in

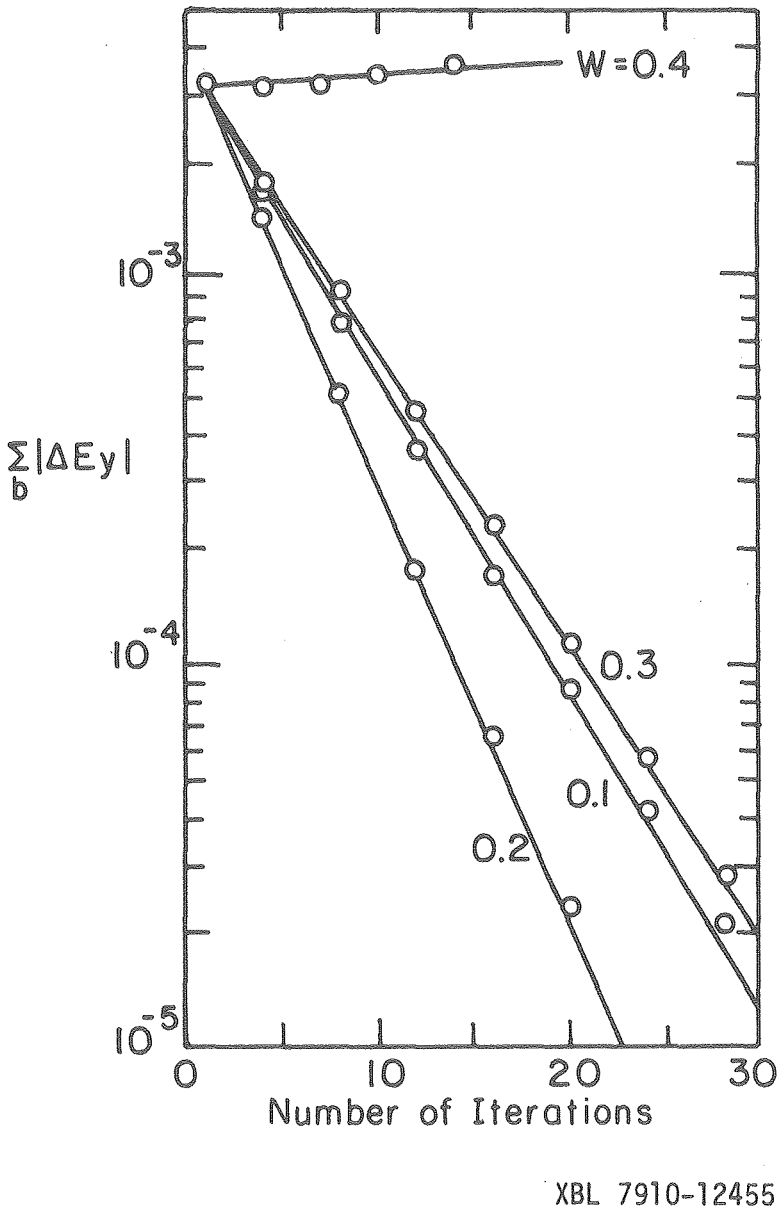

Figure 1. Convergence diagram.

x,y, and z respectively buried at a depth of 1 km in a uniform half space of 100 ohm-m resistivity. The resistivity of the body is 5 ohm-m, and the frequency used is 1.0 Hz. The incident field is a TE mode plane wave of amplitude E_y = 1.0 volts/meter. Figure 1 shows the sum of the absolute changes in E_y versus the number of iterations for different weighting coefficients. For this particular model the solution converges fastest when the coefficient is 0.2. The test allowed us to deduce a general rule of thumb which may or may not be applied to another model of different conductivity contrast. All the model results presented in this paper have been obtained using a weighting coefficient of 4.0 divided by the conductivity contrast (20, for the test model) of each model.

For an additional convergence check, a number of solutions have been obtained for an MT model by changing the number of cells employed. The model is a conductive brick of 1 km x 2 km x 2 km in size buried in a uniform half space of 100 ohm-m resistivity. The depth from the surface to the top of the body is 0.5 km, and the resistivity of the body is 0.5 ohm-m. The incident field is a plane wave with the electric field polarized either in the y-direction (TE mode) or in the x-direction (TM mode). At a frequency of 0.01 Hz, the apparent resistivity profiles obtained for the TE mode incident and the TM mode incident have been plotted in Figures 2 and 3, respectively. Each figure contains three profiles obtained using a varying number of cells: 40, 105, and 168. The convergence is reasonably good even though the conductivity contrast of the model is relatively high.

Results and applications

The electromagnetic response of several models have been obtained with the iterative hybrid scheme. The source used is a magnetic dipole

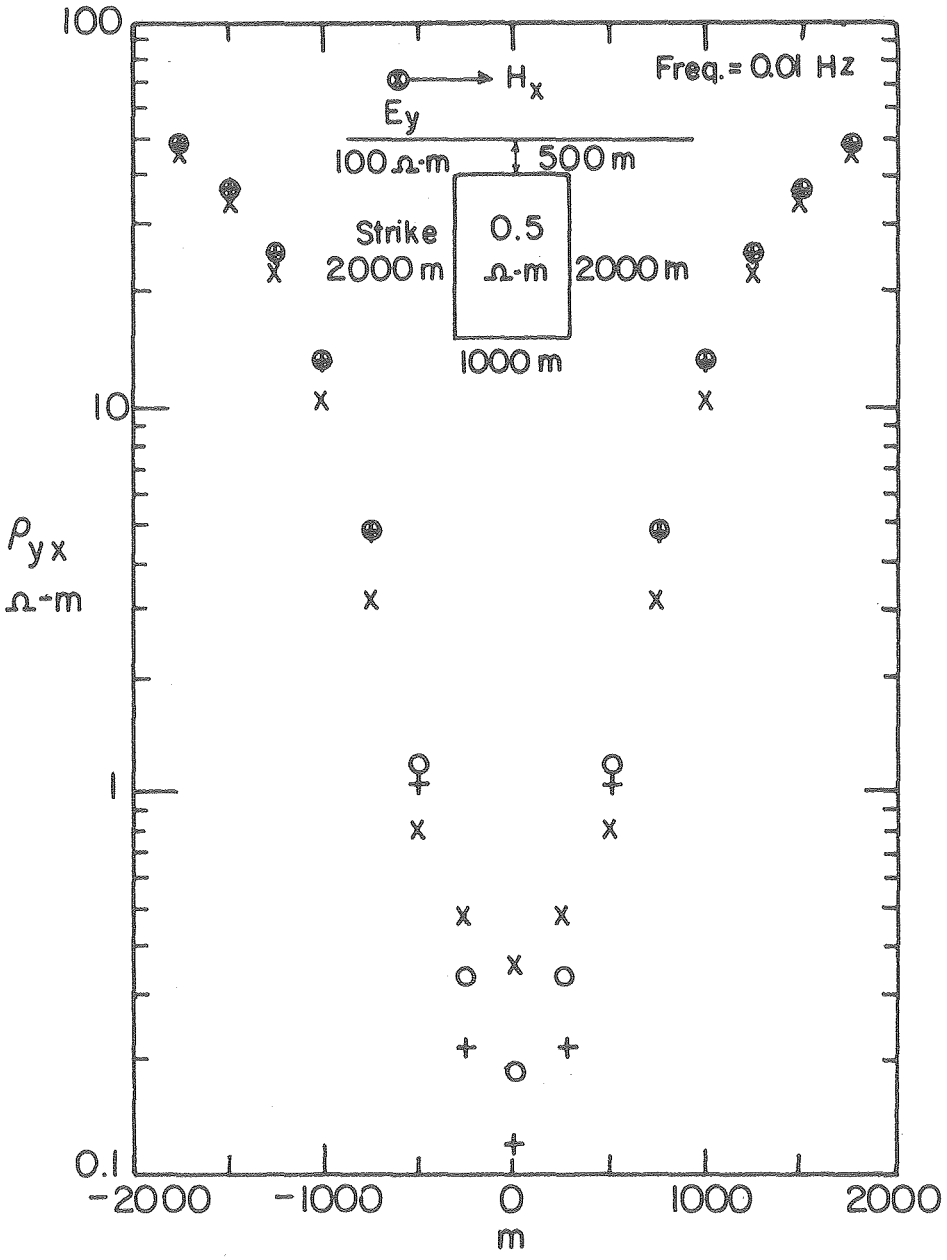

Figure 2. Apparent resistivity, ρ_{xy}, for the conductive brick model, plotting symbols reference to number of cells used in the calculation, x = 40, + = 105, 0 = 168.

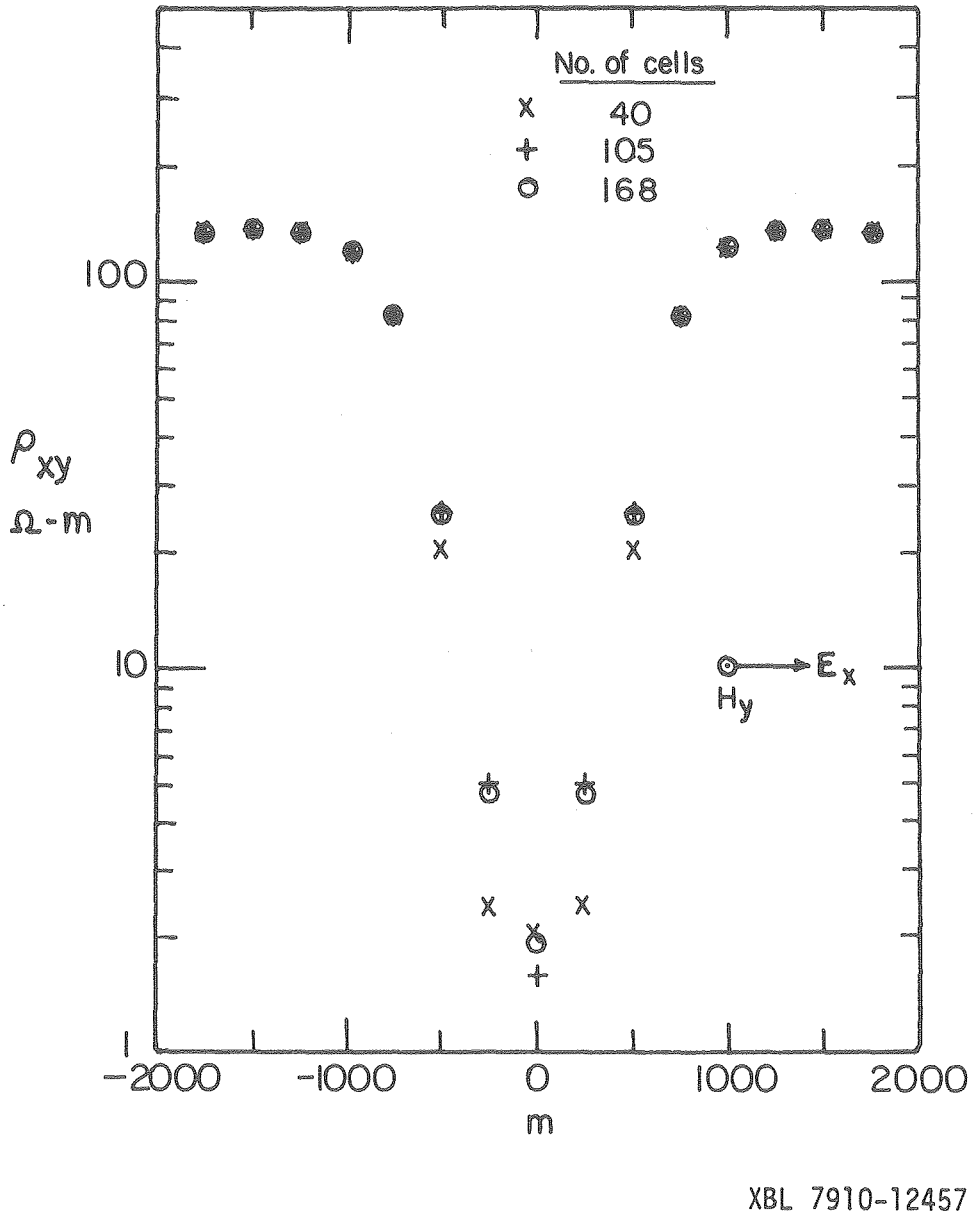

Figure 3. Apparent resistivity, ρ_{xy}, for the conductive brick model.

located on or above the surface of the earth. The required number of iterations differs from one model to the other, but has been between 30 and 50.

The first model considered is a scale tank model, the analog result of which was reported by Frishknecht (1975). The model consists of a 1.82 ohm-m conductor of size 500 m x 3,000m x 500 m buried in a uniform half space of 13.7 ohm-m resistivity. The depth to the top of the body is 200 m. An array of horizontal loops separated by 2,000 m is moved on the surface of the earth across the top of the center of the body. The frequency used is 0.15 Hz. The in-phase and quadrature parts of the normalized H_z versus the array center have been plotted in Figure 4. The hybrid solution appears to have a maximum in-phase anomaly of twice as much as that shown by the tank model. The symmetric peaks in the quadrature response on the sides of the anomaly are not observed in the hybrid solution. The integral equation solution obtained for the same model (Meyer, 1977) also failed to show these peaks. This may indicate a certain limitation of 3D numerical techniques in general. The current induced in the half space channels in and out of the body in a manner essentially similar to DC. Independent from the channelling current, an eddy current is induced in the body and tends to be concentrated along the surface of the body and may have a steeper gradient. Hence, using a limited number of elements simulating a three-dimensional body, accurate solutions for the fields associated with these induction currents would be difficult to obtain. Considering another aspect of interpretational geophysics, the typical numerical error shown in Figure 4 would not cause serious problems, i.e., the errors contained in field data would be usually greater than this, at least in the quadrature case.

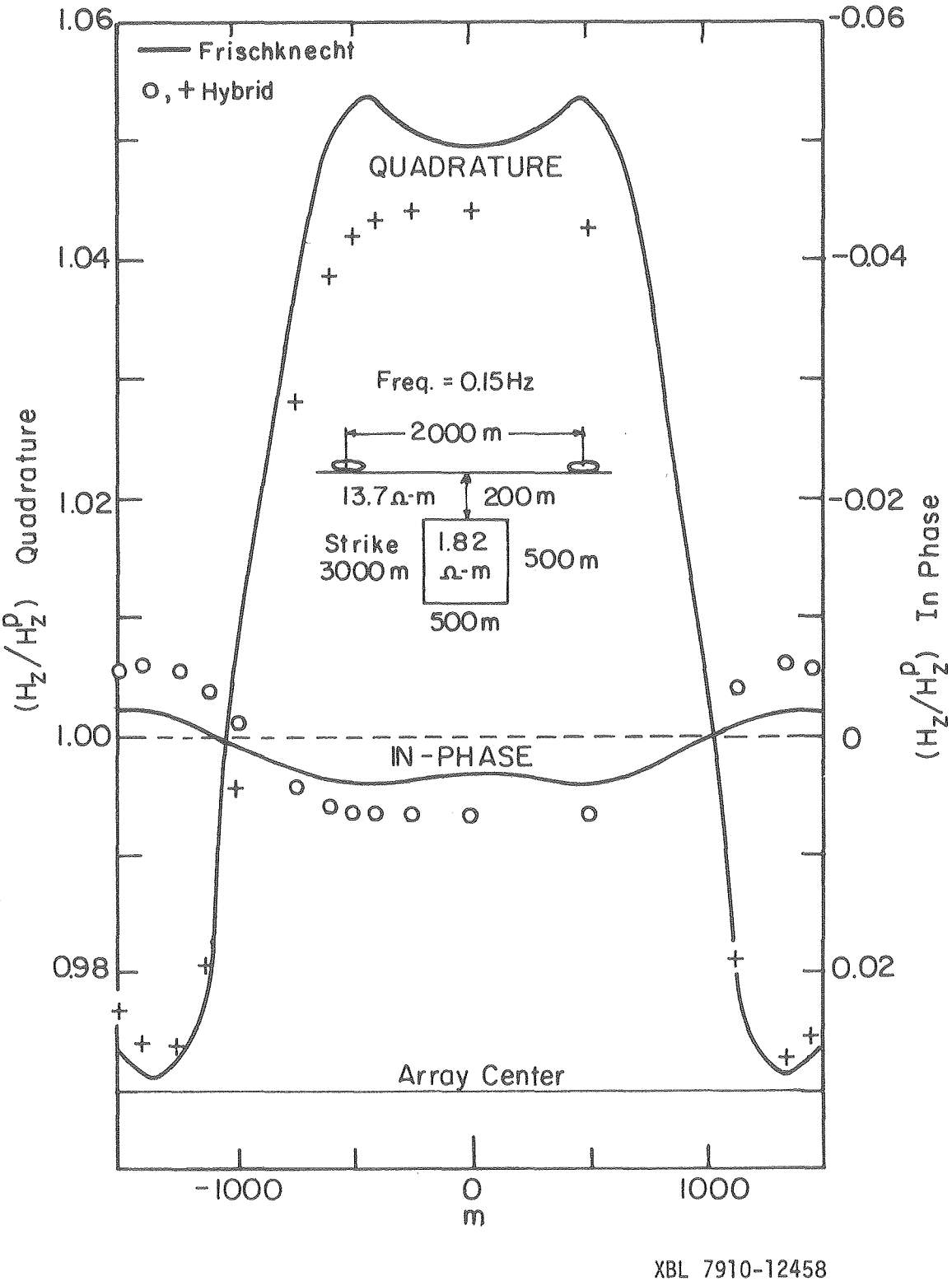

Figure 4. Comparison between the Frischknecht's scale tank model result and the hybrid solution.

The next model is a 1 ohm-m conductor of size 30 m × 120 m × 90 m buried at a depth of 30 m in a uniform half space of 30 ohm-m resistivity. A vertical magnetic dipole of moment 4π Amp-turn-meter^2 is located on the surface of the earth 75 m to the left of the center of the body. The frequency used is 1,000 Hz. The vertical component of the secondary magnetic field, H_z^s, was normalized by the free space vertical magnetic field, H_z^p, and the result has been plotted in Figure 5. At the end of the 30th iteration the average change in the boundary values became less than 0.1 percent. Along with the hybrid solution, a finite element solution has been plotted and compared. The electric field was initially obtained using the point iterative method on a system of finite element equations, and then the magnetic field was computed using Green's functions (Pridmore, 1978). The quadrature part of H_z^s shows good agreement between the solutions. The agreement is relatively poor for the in-phase.

The last model of interest is a 5 ohm-m conductive brick buried in an earth of 100 ohm-m resistivity with a 25m-thick overburden layer of 30 ohm-m resistivity. The depth to the top of the body is 50 m and the size of the body is 50 m × 250 m × 200 m. A single coil, with its magnetic moment oriented in the x-direction, is flown 50 m above the ground across the center of the body in the direction parallel to the x-axis. The frequency used is 30 Hz. The solution for this model has been obtained for use in the study of an airborne superconducting single coil system (Morrison, et al., 1976). The outline of the theory is that the secondary field produced by a conductive half space, with or without inhomogeneities, can be measured in terms of the changes in input impedance, Z, of the transmitting coil itself. The secondary

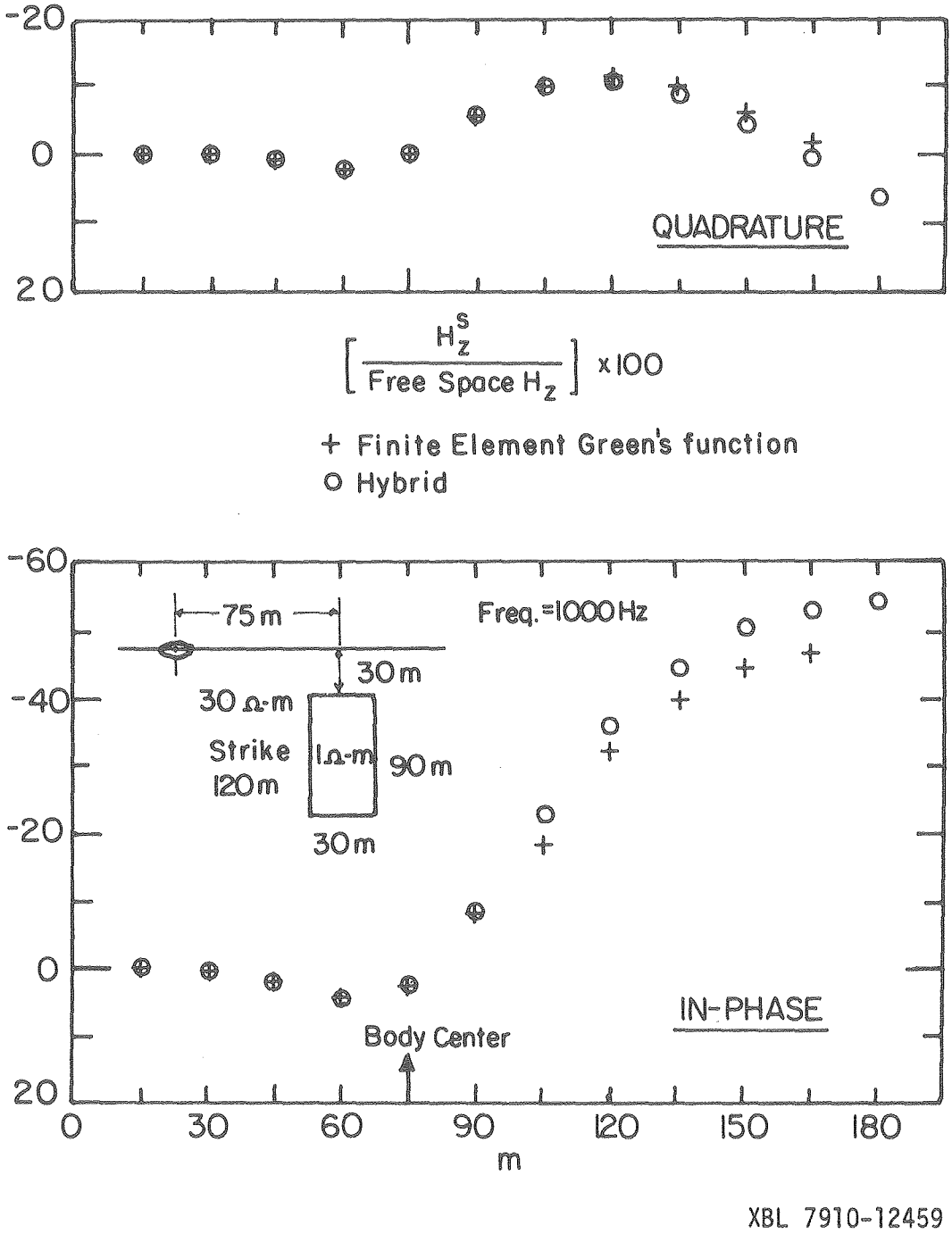

Figure 5. Comparison of the normalized H_z^s between the finite element solution and the hybrid solution for a conductive brick; data plotter at the point of the receiver coil.

magnetic field induces small voltage in the transmitter of

$$\Delta V = -N \frac{d}{dt} \int_s \bar{B} \cdot d\bar{s}$$

where N is the number of turns. Considering that the secondary field at the transmitter is locally uniform, and that only H_x contributes to the dot product $\bar{B} \cdot d\bar{s}$, the change in the voltage can be rewritten as

$$\Delta V = -j\omega\mu NAH_x$$

where A is the cross-sectional area of the coil. Since the secondary magnetic field is proportional to the magnetic moment (NIA) of the transmitter, the ΔV may be computed by

$$\Delta V = -j\omega\mu (NA)^2 I\tilde{H}_x$$

where $\tilde{H}_x$ is defined as the secondary H_x due to a unit magnetic moment. The change in the voltage in turn creates a change in the input impedance of the transmitter such that $\Delta Z = \Delta R + j\omega\Delta L = \Delta V/I$. Matching the real and imaginary parts of the ΔV separately, we find

$$\Delta R = \omega\mu (NA)^2 \mathrm{Im}(\tilde{H}_x)$$

and

$$\Delta L = -\mu (NA)^2 \mathrm{Re}(\tilde{H}_x).$$

The plots shown in Figure 6 are the in-phase and quadrature parts of $\tilde{H}_x$ computed at the transmitter, i.e., the magnetic moment used is 1.0 Amp-turn-meter^2, or alternatively NA = I = 1. At operating frequency of 30 cycles/sec. the single coil would experience a resistance change of 3.15×10^{-13} ohms from the background level to the peak of anomaly in less than 100 m. The change in inductance, however, would be a maximum of 1.07×10^{-17} henries in roughly the same distance. Assuming that a

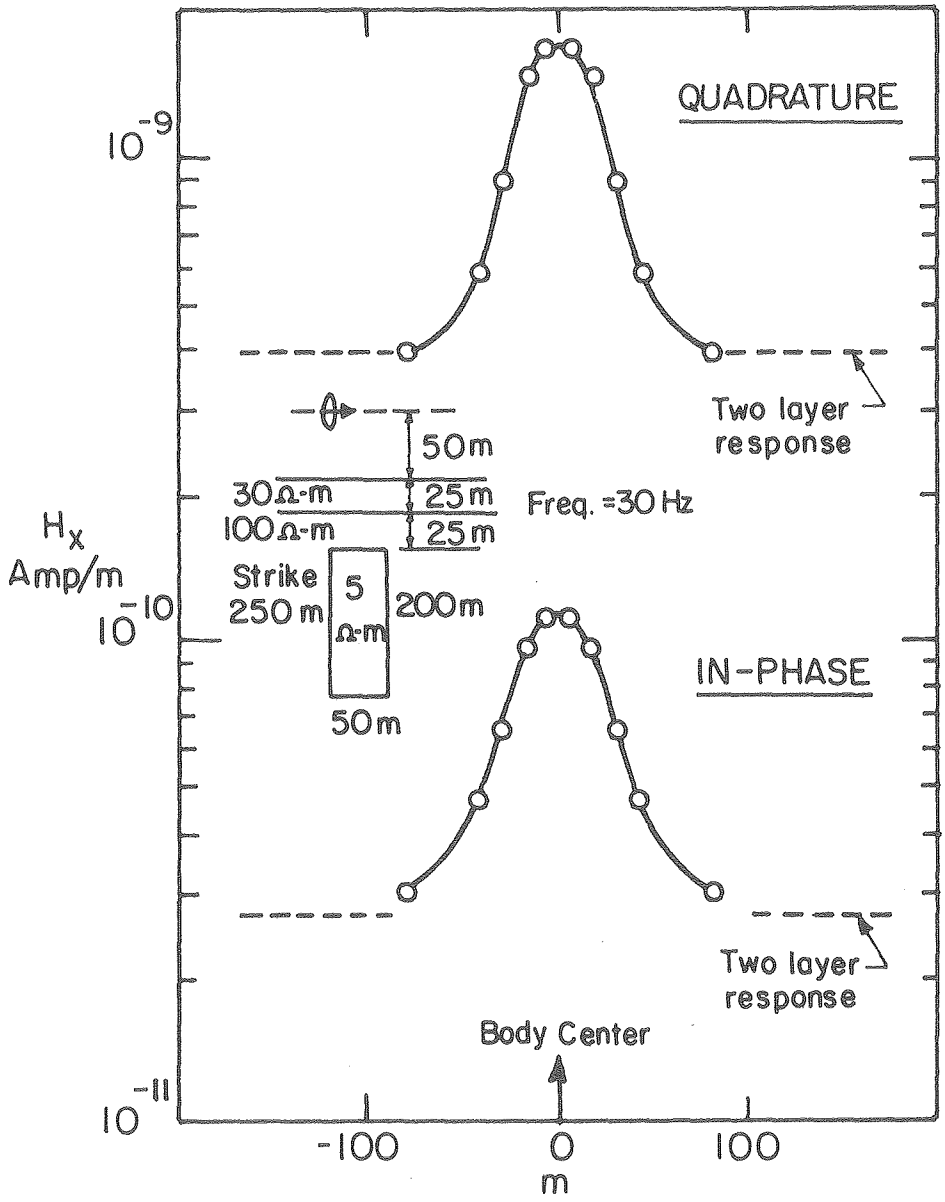

XBL 7910-12461

Figure 6. Anomalous electromagnetic response in H_x^s of a concealed conductor within the second layer of a two-layer earth, calculated at the point of the single coil.

superconducting coil possesses an $(NA)^2$ of 10^8 and that the system is capable of detecting 10^{-6} ohms with a system noise of roughly the same magnitude, the anomaly in ΔR would be 3.15×10^{-5} ohms and the signal to noise would be approximately 30. It would be difficult, if not impossible, to measure the in-phase anomaly of 1.07×10^{-9} henries.

Discussion of methods and conclusions

A numerical solution for the 3D electromagnetic problem can be obtained using either the direct or iterative hybrid scheme. The same number of Green's functions has to be evaluated in either approach. For a typical iterative solution, more than a half of the total CP time was spent for the evaluation of Green's functions. The iterative scheme solves a system of finite element equations whose matrix is banded and symmetric, but it takes a considerable number of iterations to obtain a solution. Consider a finite element mesh consists of 20 nodes in each direction. The number of unknowns (n) inside of the boundary is 17,496, and the number of unknowns (m) at the boundary is 6,504. The maximum half bandwidth (ℓ) of the finite element system matrix is 1,266. The number of complex multiplications required for a direct solution would be $0.5 \times n^3$, or 2.68×10^{12}, excluding the number for the evaluation of Green's functions. An iterative solution would require $0.5 \times n \times (\ell+1) \times (\ell+2)$ operations for the initial decomposition of the finite element matrix, plus $2 \times n \times (\ell+1) + 3 \times m \times n$ operations for the back substitution and boundary value computation per each iteration. The sum is roughly $1.41 \times 10^{10} + 3.85 \times 10^8 \times N$ at the end of the N^{th} iteration. Theoretically, the iterative scheme should be more cost-effective than the direct hybrid scheme if N is kept less than 6,900. Unfortunately, this is not the case in practice. Extensive use of extended memories

(disk) forces the iterative scheme to be severely I/O bound, and consequently the advantage of the scheme becomes much smaller than expected.

In the direct hybrid scheme, the boundary values are initially expressed in terms of the internal unknowns using an integral relation and then substituted into the finite element equations resulting in a set of combined equations. The solutions to these combined equations are the fields inside the finite element boundary.

Some analysis shows that a more cost-effective direct hybrid scheme can be easily formulated. Substituting the internal unknowns $\underline{E}_s^i$, equation (21), into equation (17), we obtain

$$\underline{E}_s^b = -GK_{ii}^{-1}(K_{ib}\underline{E}_s^b + S_i) + S_p \tag{23}$$

then the direct solution for the boundary value $\underline{E}_s^b$ becomes

$$\underline{E}_s^b = (I_m + GK_{ii}^{-1}K_{ib})^{-1}(S_p - GK_{ii}^{-1}S_i) \tag{24}$$

where I_m is an m×m identity matrix. The scattered fields elsewhere can then be obtained by initially calculating the fields inside of the boundary using equation (21) and then carrying out necessary volume integrations. In terms of the number of operations, the ratio of the earlier direct hybrid scheme to the one we have shown would be roughly $(n/m)^3$. Depending upon the ratio (n/m) of a given model, a substantial amount of computing time could be saved using the new scheme. For the same mesh described earlier in this section the ratio, $(n/m)^3$, would be approximately 19, a saving of at least a factor of 10.

Acknowledgements

This research has been supported by a grant from Amax Exploration, Inc. The computer modelling has been supported in part by the U. S. Department of Energy, Division of Geothermal Energy under Contract W-7405-ENG-48 to the Lawrence Berkeley Laboratory and the University of California, Berkeley.

The authors would like to acknowledge Dr. William Scheen of Royal Dutch Shell for his hybrid scheme algorithm, presented at the Electromagnetic Workshop held at the Lawrence Berkeley Laboratory, 1978.

References

Frischknecht, F. C. 1967, Fields about an oscillating magnetic dipole over a two-layer earth, and application to ground and airborne electromagnetic surveys, Quarterly of the Colorado School of Mines, v. 62, no. 1.

Harrington, R. F., 1961, Time-harmonic electromagnetic fields, New York, McGraw Hill.

Hohmann, G. W., 1975, Three-dimensional induced polarization and electromagnetic modelling, Geophysics, v. 40, p. 309-324.

Lines, L. R., and Jones, F. W., 1973, The perturbation of alternating geomagnetic fields by three-dimensional island structures, Geophys. J. R. ast. Soc., v. 32, p. 133-154.

Meyer, W. H., 1977, Computer modelling of electromagnetic prospecting methods, Berkeley, Ph.D. Thesis, University of California.

Morrison, H. F., Dolan, W., and Dey, A., 1976, Earth conductivity determinations employing a single superconducting coil, Geophysics, v. 41, p. 1184-1206.

Morse, P. M., Feshbach, H., 1953, Methods of theoretical physics, New York, McGraw Hill.

Pridmore, D. F., 1978, Three-dimensional modelling of electric and electromagnetic data using the finite element method, Ph.D. Thesis, The University of Utah.

Quon, C., 1963, Electromagnetic fields of elevated dipoles on a two-layer earth, M.S. Thesis, University of Alberta.

Reddy, I. K., Rankin, D., and Phillips, R. J., 1977, Three-dimensional modelling in magnetotelluric and magnetic variational sounding, Geophys. J. R. ast. Soc., v. 51, p. 313-326.

Reid, J. K., 1972, Two fortran subroutines for direct solution of linear equations whose matrix is sparse, symmetric, and positive-definite, U.K.A.E.A. Research Group Report AERE-R7119.

Scheen, W. L., 1978, EMMMMA, A computer program for three-dimensional modelling of airborne electromagnetic surveys, Proc. Workshop on modelling of electrical and electromagnetic methods, LBL-7053, p. 53.

Stakgold, I., 1968, Boundary value problems of mathematical physics, v. II, New York, Macmillan.

Wait, J. R., 1962, Electromagnetic waves in stratifield media, New York, Macmillan.

Weidelt, P., 1975, Electromagnetic induction in three-dimensional structures, J. Geophysics, v. 41, p. 85-109.

Zienkiewicz, O. C., 1971, The finite element method in engineering science, New York, McGraw Hill.

Appendix

Electromagnetic Fields Due to a Current Source Embedded in a Lower Half Space of a Two-Layered Earth

Using the Sommerfeld integral, we can rewrite the particular solution $\bar{A}^p$, equation (12), as

$$\bar{A}^p = \frac{\bar{J}^s}{4\pi} \int_0^\infty \frac{\lambda}{u_2} e^{-u_2|z-z'|} J_0(\lambda\rho)d\lambda \tag{A-1}$$

where $u_i = (\lambda^2 - k_i^2)^{1/2}$ and $\rho = \{(x-x')^2 + (y-y')^2\}^{1/2}$. The horizontal wave number λ is given by $\lambda = (k_x^2+k_y^2)^{1/2}$, where k_x and k_y are the wave numbers in x and y, respectively. Using relation (Banos, 1966)

$$\iint_{-\infty}^{\infty} f(k_x^2+k_y^2) e^{j\{k_x(x-x')+k_y(y-y')\}} dk_x dk_y = 2\pi \int_0 \lambda f(\lambda)\ J_0(\lambda\rho)d\lambda$$

we find

$$\bar{A}^p(k_x,k_y,z) = \frac{\bar{J}^s}{2} \frac{e^{-u_2|z-z'|}}{u_2} \tag{A-2}$$

in Fourier transform space. The vertical components of corresponding primary fields are

$$E_z^p(k_x,k_y,z) = \frac{jk_x}{\hat{y}_2} \frac{J_x}{2} \frac{\partial}{\partial z} \frac{e^{-u_2|z-z'|}}{u_2}$$

$$H_z^p(k_x,k_y,z) = -jk_y \frac{J_x}{2} \frac{e^{-u_2|z-z'|}}{u_2} \tag{A-3}$$

for $\bar{J}^s = \bar{i}_x J_x$, and

$$E_z^p(k_x,k_y,z) = \frac{jk_y}{y_2} \frac{J_y}{2} \frac{\partial}{\partial z} \frac{e^{-u_2|z-z'|}}{u_2}$$

$$H_z^p(k_x,k_y,z) = jk_z \frac{J_y}{2} \frac{e^{-u_2|z-z'|}}{u_2} \tag{A-4}$$

for $\bar{J}^s = \bar{i}_y J_y$, and

$$E_z^p(k_x,k_y,z) = \frac{\lambda^2}{\hat{y}_2}\frac{J_z}{2}\frac{e^{-u_2|z-z'|}}{u_2}$$

$$H_z^p(k_x,k_y,z) = 0 \qquad \text{(A-5)}$$

for $\bar{J}^s = \bar{i}_z J_z$.

In a homogeneous source-free region, the rectangular components of vector potential $\bar{A}$ and $\bar{F}$ satisfy Helmholtz equation (Harrington, 1961, p. 129)

$$\nabla^2\psi + k^2\psi = 0. \qquad \text{(A-6)}$$

The electric and magnetic fields due to these potentials are given by

$$\bar{E} = -\nabla\times\bar{F} - \hat{z}\bar{A} + \frac{1}{\hat{y}}\nabla(\nabla\cdot\bar{A})$$

$$\bar{H} = \nabla\times\bar{A} - \hat{y}\bar{F} + \frac{1}{\hat{z}}\nabla(\nabla\cdot\bar{F}). \qquad \text{(A-7)}$$

By inspection, there will be no E_z if we choose $\bar{A} = 0$ and $\bar{F} = \bar{i}_z\theta$. On the other hand, if we choose $\bar{A} = \bar{i}_z\phi$ and $\bar{F} = 0$, there will be no H_z. A field with no E_z is called transverse electric to z (TE), and a field with no H_z is called transverse magnetic to z (TM). Superposing these two independent modes, one can completely express an arbitrary field, $\bar{E}$ and $\bar{H}$, in the source free region.

In the presence of a two-layered half space, θ and ϕ satisfy equation (A-6) and the solutions in Fourier transform space will be

$$\begin{pmatrix}\theta_i\\ \phi_i\end{pmatrix} = \begin{pmatrix}\theta_i^+\\ \phi_i^+\end{pmatrix} e^{-u_i z - u_2 z'} + \begin{pmatrix}\theta_i^-\\ \phi_i^-\end{pmatrix} e^{u_i z - u_2 z'}, \quad i = 0,1,2. \qquad \text{(A-8)}$$

In its present coordinate system with z positive down, the supersign "+" denotes downgoing potential. Since there is no downgoing potential in the air, $\theta_0^+ = \phi_0^+ = 0$. The upgoing potentials, θ_2^- and ϕ_2^-, in the

lower half space are the primary terms due to the current element in that region. The electric and magnetic fields are then expressed in terms of θ and ϕ as

$$E_x = -\frac{\partial\theta}{\partial y} + \frac{1}{\hat{y}}\frac{\partial^2\phi}{\partial x\partial z}$$

$$E_y = \frac{\partial\theta}{\partial x} + \frac{1}{\hat{y}}\frac{\partial^2\phi}{\partial y\partial z} \qquad \text{(A-9)}$$

$$E_z = -\hat{z}\phi + \frac{1}{\hat{y}}\frac{\partial^2\phi}{\partial z^2} = \frac{\lambda^2}{\hat{y}}\phi$$

and

$$H_x = \frac{\partial\phi}{\partial y} + \frac{1}{\hat{z}}\frac{\partial^2\theta}{\partial x\partial z}$$

$$H_y = -\frac{\partial\phi}{\partial x} + \frac{1}{\hat{z}}\frac{\partial^2\theta}{\partial y\partial z} \qquad \text{(A-10)}$$

$$H_z = -\hat{y}\theta + \frac{1}{\hat{z}}\frac{\partial^2\theta}{\partial z^2} = \frac{\lambda^2}{\hat{z}}\theta.$$

Equations (A-9) and (A-10) show that E_z depends only on ϕ and H_z only on θ. Equating the primary fields E_z^p and H_z^p given by (A-3), (A-4), and (A-5) to E_z and H_z in equations (A-9) and (A-10) with potentials θ and ϕ substituted by the upgoing primary potentials $\theta_2^- e^{u_2 z - u_2 z'}$ and $\phi_2^- e^{u_2 z - u_2 z'}$, we obtain

$$\theta_2^- = -\frac{jk_y}{\lambda^2}\frac{\hat{z}_2 J_x}{2}\frac{1}{u_2}$$

$$\phi_2^- = \frac{jk_x}{\lambda^2}\frac{J_x}{2} \qquad \text{(A-11)}$$

for $\bar{J}^s = \bar{i}_x J_x$, and

$$\theta_2^- = \frac{jk_x}{\lambda^2}\frac{\hat{z}_2 J_y}{2}\frac{1}{u_2}$$

$$\phi_2^- = \frac{jk_y}{\lambda^2}\frac{J_y}{2} \qquad \text{(A-12)}$$

for $\bar{J}^s = \bar{i}_y J_y$, and

$$\theta_2^- = 0$$

$$\phi_2^- = \frac{J_z}{2}\frac{1}{u_2} \tag{A-13}$$

for $\bar{J}^s = \bar{i}_z J_z$.

The next step is to find coefficients θ_0^-, θ_1^+, θ_1^-, and θ_2^+ for the TE mode, and ϕ_0^-, ϕ_1^+, ϕ_1^-, and ϕ_2^+ for the TM mode. These coefficients are determined by matching boundary conditions for tangential components of $\bar{E}$ and $\bar{H}$ at layer boundaries. The principle of superposition suggests that boundary conditions may be applied to each mode separately. Thus, from the boundary conditions for the TE mode, we find

$$\theta_0^- = \frac{4N_1N_2e^{u_2d}}{(N_1+N_0)(N_2+N_1)e^{u_1d}+(N_1-N_0)(N_2-N_1)e^{-u_1d}}\theta_2^-$$

$$\theta_1^+ = \frac{2N_2(N_1-N_0)e^{u_2d}}{(N_1+N_0)(N_2+N_1)e^{u_1d}+(N_1-N_0)(N_2-N_1)e^{-u_1d}}\theta_2^- \tag{A-14}$$

$$\theta_1^- = \frac{2N_2(N_1+N_0)e^{u_2d}}{(N_1+N_0)(N_2+N_1)e^{u_1d}+(N_1-N_0)(N_2-N_1)e^{-u_1d}}\theta_2^-$$

$$\theta_2^+ = \frac{(N_1+N_0)(N_2-N_1)e^{u_1d}+(N_1-N_0)(N_2+N_1)e^{-u_1d}}{(N_1+N_0)(N_2+N_1)e^{u_1d}+(N_1-N_0)(N_2-N_1)e^{-u_1d}}e^{2u_2d}\theta_2^-$$

where d is the thickness of the first layer and $N_i = \frac{u_i}{\hat{z}_i}$. The coefficients for the TM mode have expressions identical to (A-14) with θ_i and N_i substituted by ϕ_i and $K_i(=\frac{u_i}{\hat{y}_i})$. Replacing jk_x by $\frac{\partial}{\partial x}$ and jk_y by $\frac{\partial}{\partial y}$ and using equation (A-7) for $\bar{E}$ and $\bar{H}$, we obtain the following electric and

magnetic fields in the region of interest. Hereafter, ϕ_i and θ_i represent only the coefficient part of the potentials given by equation (A-14).

a. Electric fields in the lower half space

$$E_x^2 = E_x^p + \frac{1}{4\pi}\int_0^\infty e^{-u_2(z+z')}\,d\lambda\cdot$$

$$J_x\Big[\frac{1}{\hat{x}_2}\Big\{\Big(-\frac{2(x-x')^2}{\rho^3}+\frac{1}{\rho}\Big)J_1(\lambda\rho)+\frac{(x-x')^2}{\rho^2}\lambda J_0(\lambda\rho)\Big\}\phi_2^+u_2$$

$$+\hat{z}_2\Big\{\Big(\frac{2(y-y')^2}{\rho^3}-\frac{1}{\rho}\Big)J_1(\lambda\rho)-\frac{(y-y')^2}{\rho^2}\lambda J_0(\lambda\rho)\Big\}\theta_2^+\frac{1}{u_2}\Big]$$

$$+J_y\Big[\frac{1}{\hat{y}_2}\Big\{-\frac{2(x-x')(y-y')}{\rho^3}J_1(\lambda\rho)+\frac{(x-x')(y-y')}{\rho^2}\lambda J_0(\lambda\rho)\Big\}\phi_2^+u_2$$

$$+\hat{z}_2\Big\{-\frac{2(x-x')(y-y')}{\rho^3}J_1(\lambda\rho)+\frac{(x-x')(y-y')}{\rho^2}\lambda J_0(\lambda\rho)\Big\}\theta_2^+\frac{1}{u_2}\Big]$$

$$+J_z\Big[\frac{1}{\hat{y}_2}\frac{(x-x')}{\rho}\lambda^2J_1(\lambda\rho)\phi_2^+\Big]$$

$$E_y^2 = E_y^p + \frac{1}{4\pi}\int_0^\infty e^{-u_2(z+z')}\,d\lambda\cdot$$

$$J_x\Big[\frac{1}{\hat{y}_2}\Big\{-\frac{(x-x')(y-y')}{\rho^3}J_1(\lambda\rho)+\frac{(x-x')(y-y')}{\rho^2}\lambda J_0(\lambda\rho)\Big\}\phi_2^+u_2$$

$$+\hat{z}_2\Big\{-\frac{(x-x')(y-y')}{\rho^3}J_1(\lambda\rho)+\frac{(x-x')(y-y')}{\rho^2}\lambda J_0(\lambda\rho)\Big\}\theta_2^+\frac{1}{u_2}\Big] \qquad \text{(A-15)}$$

$$+J_y\Big[\frac{1}{\hat{y}_2}\Big\{\Big(-\frac{2(y-y')^2}{\rho^3}+\frac{1}{\rho}\Big)J_1(\lambda\rho)+\frac{(y-y')^2}{\rho^2}\lambda J_0(\lambda\rho)\Big\}\phi_2^+u_2$$

$$+\hat{z}_2\Big\{\Big(\frac{2(x-x')^2}{\rho^3}-\frac{1}{\rho}\Big)J_1(\lambda\rho)-\frac{(x-x')^2}{\rho^2}\lambda J_0(\lambda\rho)\Big\}\theta_2^+\frac{1}{u_2}\Big]$$

$$+J_z\Big[\frac{1}{\hat{y}_2}\frac{(y-y')}{\rho}\lambda^2J_1(\lambda\rho)\phi_2^+\Big]$$

$$E_z^2 = E_z^p + \frac{1}{4\pi}\int_0^\infty e^{-u_2(z+z')}\,d\lambda\cdot$$

$$J_x\Big[\frac{1}{\hat{y}_2}\Big(-\frac{x-x'}{\rho}\Big)\lambda^2J_1(\lambda\rho)\phi_2^+\Big]$$

$$+J_y\Big[\frac{1}{\hat{y}_2}\Big(-\frac{y-y'}{\rho}\Big)\lambda^2J_1(\lambda\rho)\phi_2^+\Big]$$

$$+ J_z[\frac{1}{\hat{y}_2} \lambda^3 J_0(\lambda\rho)\phi_2^+ \frac{1}{u_2}],$$

where the primary fields E_x^p, E_y^p, and E_z^p are due to the primary potentials θ_2^- and ϕ_2^-. Since these potentials are identical to the primary potential $\bar{A}^p$ given by equation (12), the primary electric fields may be analytically obtained using equation (13).

b. Electric fields in the layer

$$E_x^1 = \frac{1}{4\pi} \int_0^\infty e^{-u_2 z'} d\lambda.$$

$$J_x[\frac{1}{\hat{y}_1} \{(- \frac{2(x-x')^2}{\rho^3} + \frac{1}{\rho}) J_1(\lambda\rho) + \frac{(x-x')^2}{\rho^2} \lambda J_0(\lambda\rho)\}(\phi_1^+ e^{-u_1 z} - \phi_1^- e^{u_1 z})u_1$$

$$+ \hat{z}_1\{(\frac{2(y-y')^2}{\rho^3} - \frac{1}{\rho}) J_1(\lambda\rho) - \frac{(y-y')^2}{\rho^2} \lambda J_0(\lambda\rho)\}(\theta_1^+ e^{-u_1 z} + \theta_1^- e^{u_1 z}) \frac{1}{u_2}]$$

$$+ J_y[\frac{1}{\hat{y}_1}\{- \frac{2(x-x')(y-y')}{\rho^3} J_1(\lambda\rho) + \frac{(x-x')(y-y')}{\rho^2} \lambda J_0(\lambda\rho)\}(\phi_1^+ e^{-u_1 z} - \phi_1^- e^{u_1 z})u_1$$

$$+ \hat{z}_1\{- \frac{2(x-x')(y-y')}{\rho^3} J_1(\lambda\rho) + \frac{(x-x')(y-y')}{\rho^2} \lambda J_0(\lambda\rho)\}(\theta_1^+ e^{-u_1 z} + \theta_1^- e^{u_1 z}) \frac{1}{u_2}]$$

$$+ J_z[\frac{1}{\hat{y}_1} \frac{(x-x')}{\rho} \lambda^2 J_1(\lambda\rho)(\phi_1^+ e^{-u_1 z} - \phi_1^- e^{u_1 z}) \frac{u_1}{u_2}]$$

$$E_y^1 = \frac{1}{4\pi} \int_0^\infty e^{-u_2 z'} d\lambda.$$

$$J_x[\frac{1}{\hat{y}_1} \{- \frac{2(x-x')(y-y')}{\rho^3} J_1(\lambda\rho) + \frac{(x-x')(y-y')}{\rho^2} \lambda J_0(\lambda\rho)\}(\phi_1^+ e^{-u_1 z} - \phi_1^- e^{u_1 z})u_1$$

$$+ \hat{z}_1\{- \frac{2(x-x')(y-y')}{\rho^3} J_1(\lambda\rho) + \frac{(x-x')(y-y')}{\rho^2} \lambda J_0(\lambda\rho)\}(\theta_1^+ e^{-u_1 z} + \theta_1^- e^{u_1 z}) \frac{1}{u_2}]$$

$$+ J_y[\frac{1}{\hat{y}_1} \{(- \frac{2(y-y')^2}{\rho^3} + \frac{1}{\rho}) J_1(\lambda\rho) + \frac{(y-y')^2}{\rho^2} \lambda J_0(\lambda\rho)\}(\phi_1^+ e^{-u_1 z} - \phi_1^- e^{u_1 z})u_1$$

$$+ \hat{z}_1\{(\frac{2(x-x')^2}{\rho^3} - \frac{1}{\rho}) J_1(\lambda\rho) - \frac{(x-x')^2}{\rho^2} \lambda J_0(\lambda\rho)\}(\theta_1^+ e^{-u_1 z} + \theta_1^- e^{u_1 z}) \frac{1}{u_2}]$$

$$+ J_z[\frac{1}{\hat{y}_1} \frac{(y-y')}{\rho} \lambda^2 J_1(\lambda\rho)(\phi_1^+ e^{-u_1 z} - \phi_1^- e^{u_1 z}) \frac{u_1}{u_2}] \qquad \text{(A-16)}$$

$$E_z^1 = \frac{1}{4\pi}\int_0^\infty e^{-u_2 z'}\, d\lambda.$$

$$J_x\left[\frac{1}{\hat{y}_1}\left(-\frac{x-x'}{\rho}\right)\lambda^2 J_1(\lambda\rho)\left(\phi_1^+ e^{-u_1 z} + \phi_1^- e^{u_1 z}\right)\right]$$

$$+ J_y\left[\frac{1}{\hat{y}_1}\left(-\frac{y-y'}{\rho}\right)\lambda^2 J_1(\lambda\rho)\left(\phi_1^+ e^{-u_1 z} + \phi_1^- e^{u_1 z}\right)\right]$$

$$+ J_z\left[\frac{1}{\hat{y}_1}\lambda^3 J_0(\lambda\rho)\left(\phi_1^+ e^{-u_1 z} + \phi_1^- e^{u_1 z}\right)\frac{1}{u_2}\right].$$

c. Magnetic fields in the air

$$H_x^0 = \frac{1}{4\pi}\int_0^\infty e^{u_0 z - u_2 z'}\, d\lambda.$$

$$J_x\left[\left\{\frac{2(x-x')(y-y')}{\rho^3} J_1(\lambda\rho) - \frac{(x-x')(y-y')}{\rho^2}\lambda J_0(\lambda\rho)\right\}\phi_0^-\right.$$

$$\left. + \left\{-\frac{2(x-x')(y-y')}{\rho^3} J_1(\lambda\rho) + \frac{(x-x')(y-y')}{\rho^2}\lambda J_0(\lambda\rho)\right\}\theta_0^-\frac{u_0}{u_2}\right]$$

$$+ J_y\left[\left\{\left(\frac{2(y-y')^2}{\rho^3} - \frac{1}{\rho}\right) J_1(\lambda\rho) - \frac{(y-y')^2}{\rho^2}\lambda J_0(\lambda\rho)\right\}\phi_0^-\right.$$

$$\left. + \left\{\left(\frac{2(x-x')^2}{\rho^3} - \frac{1}{\rho}\right) J_1(\lambda\rho) - \frac{(x-x')^2}{\rho^2}\lambda J_0(\lambda\rho)\right\}\theta_0^-\frac{u_0}{u_2}\right]$$

$$+ J_z\left[\left(-\frac{y-y'}{\rho}\right)\lambda^2 J_1(\lambda\rho)\phi_0^-\frac{1}{u_2}\right]$$

$$H_y^0 = \frac{1}{4\pi}\int_0^\infty e^{u_0 z - u_2 z'}\, d\lambda.$$

$$J_x\left[\left\{\left(-\frac{2(x-x')^2}{\rho^3} + \frac{1}{\rho}\right) J_1(\lambda\rho) + \frac{(x-x')^2}{\rho^2}\lambda J_0(\lambda\rho)\right\}\phi_0^-\right.$$

$$\left. + \left\{\left(-\frac{2(y-y')^2}{\rho^3} + \frac{1}{\rho}\right) J_1(\lambda\rho) + \frac{(y-y')^2}{\rho^2}\lambda J_0(\lambda\rho)\right\}\theta_0^-\frac{u_0}{u_2}\right]$$

$$+ J_y\left[\left\{-\frac{2(x-x')(y-y')}{\rho^3} J_1(\lambda\rho) + \frac{(x-x')(y-y')}{\rho^2}\lambda J_0(\lambda\rho)\right\}\phi_0^-\right.$$

$$\left. + \left\{\frac{2(x-x')(y-y')}{\rho^3} J_1(\lambda\rho) - \frac{(x-x')(y-y')}{\rho^2}\lambda J_0(\lambda\rho)\right\}\theta_0^-\frac{u_0}{u_2}\right]$$

$$+ J_z\left[\frac{x-x'}{\rho}\lambda^2 J_1(\lambda\rho)\phi_0^-\frac{1}{u_2}\right] \qquad \text{(A-17)}$$

$$H_z^0 = \frac{1}{4\pi} \int_0^\infty e^{u_0 z - u_2 z'} \, d\lambda .$$

$$J_x\left[\frac{y-y'}{\rho} \lambda^2 J_1(\lambda\rho)\theta_0^- \frac{1}{u_2}\right]$$

$$+ J_y\left[\left(-\frac{x-x'}{\rho}\right)\lambda^2 J_1(\lambda\rho)\theta_0^- \frac{1}{u_2}\right]$$

$$+ J_z[0].$$

The electric and magnetic fields due to a point source of current $\bar{J}^s$ can alternatively be written in a compact form as

$$\bar{E}(\bar{r}) = \bar{\bar{\Gamma}}^E(\bar{r};\bar{r}') \cdot \bar{J}^s(\bar{r}') \tag{A-18}$$

and

$$\bar{H}(\bar{r}) = \bar{\bar{\Gamma}}^H(\bar{r};\bar{r}') \cdot \bar{J}^s(\bar{r}') \tag{A-19}$$

where $\bar{\bar{\Gamma}}$ is a tensor Green's function (Harrington, 1961).

References

Banos, A., 1966, Dipole radiation in the presence of a conducting half space, New York, Pergammon Press.

Harrington, R. F., 1961, Time-harmonic electromagnetic fields, New York, McGraw Hill.